Normalization method and application for MODIS TEB assessments using Earth scene measurements

Tiejun Chang[1], Xiaoxiong Xiong[2], Ashish Shrestha[1], and Carlos Perez-Diaz[1]

[1]Science Systems and Applications, Inc.
[2]NASA Goddard Space Flight Center

November 23, 2022

Abstract

Selected Earth targets are commonly used for satellite sensor calibration assessments (e.g. sensor stability and inter-comparisons). Moreover, typical scenes used for the calibration assessment of the thermal emissive bands (TEBs) include Dome Concordia (Dome-C), ocean, desert, and deep convective clouds (DCC). Reference data used for these calibration assessments can come from another band, another instrument, or ground measurements. The Dome-C site, covered with uniformly-distributed permanent snow, is normally used for the assessment of the TEBs at cold temperatures. Furthermore, ocean and desert measurements prove useful for scenes with higher temperatures. The DCC, one of the most consistent and coldest targets, can be used for the TEBs calibration and product stability assessments. MODIS band 31 (˜ 11 mm) can be used as a reference for these scenes. However, measurements over these scenes have seasonal variations, and the DCC brightness temperatures (BTs) have asymmetrical distributions. These features can introduce additional uncertainty to the stability assessments. A normalization method is applied by using an empirical model to derive reference-dependent BTs. Using the developed empirical model, measurements can be normalized to a reference BT in order to enhance the calibration assessment's accuracy. This method is evaluated using all four scene types (i.e. ocean, desert, snow (Dome-C), and DCC) and applied to all the Terra and Aqua MODIS TEBs. Stability assessments over the instruments' entire data records are presented and discussed. The technique can be applied in future efforts to support MODIS TEBs calibration assessments.

Normalization method and application for MODIS TEB assessments using Earth scene measurements

Tiejun Chang[1], Xiaoxiong Xiong[2], Ashish Shrestha[1], and Carlos Perez Diaz[1]
[1] Science Systems and Applications, Inc., Lanham, MD 20706.
[2] Sciences and Exploration Directorate, NASA/GSFC, Greenbelt, MD 20771.

Corresponding author: Tiejun Chang (tiejun.chang@ssaihq.com)

Key points:

- A normalization method is developed to enhance the accuracy of stability assessments using Earth measurements.
- The normalization technique is applied to measurements over Dome-C, DCC, the ocean, and the desert.
- MODIS TEBs long-term stability assessments are presented and discussed.

Abstract

Selected Earth targets are commonly used for satellite sensor calibration assessments (e.g. sensor stability and inter-comparisons). Moreover, typical scenes used for the calibration assessment of the thermal emissive bands (TEBs) include Dome Concordia (Dome-C), ocean, desert, and deep convective clouds (DCC). Reference data used for these calibration assessments can come from another band, another instrument, or ground measurements. The Dome-C site, covered with uniformly-distributed permanent snow, is normally used for the assessment of the TEBs at cold temperatures. Furthermore, ocean and desert measurements prove useful for scenes with higher temperatures. The DCC, one of the most consistent and coldest targets, can be used for the TEBs calibration and product stability assessments. MODIS band 31 (~ 11 μm) can be used as a reference for these scenes. However, measurements over these scenes have seasonal variations, and the DCC brightness temperatures (BTs) have asymmetrical distributions. These features can introduce additional uncertainty to the stability assessments. A normalization method is applied by using an empirical model to derive reference-dependent BTs. Using the developed empirical model, measurements can be normalized to a reference BT in order to enhance the calibration assessment's accuracy. This method is evaluated using all four scene types (i.e. ocean, desert, snow (Dome-C), and DCC) and applied to all the Terra and Aqua MODIS TEBs. Stability assessments over the instruments' entire data records are presented and discussed. The technique can be applied in future efforts to support MODIS TEBs calibration assessments.

1 Introduction

The Terra and Aqua Moderate Resolution Imaging Spectroradiometer (MODIS) sensors have been on-orbit for more than 20 and 18 years, respectively, and have provided continuous global observations for science research and applications. On-orbit calibration updates are important to track instrument response changes and maintain data product quality. MODIS has 36 spectral bands, among which bands 20 to 25 and 27 to 36 are the thermal emissive bands (TEBs) with a wavelength range from 3.8 μm to 14.2 μm. The MODIS TEBs radiometric calibration uses a quadratic function for instrument response, and the calibration coefficients look-up tables (LUTs) are updated using its on-board blackbody's (BB) response [*Xiong et al., 2009; Xiong et al., 2015*]. On-board BB warm-up and cool-

down (WUCD) events, where the BB temperature ranges from instrument temperature (around 270 K) to 315 K, are performed quarterly. The derived nonlinear response coefficient has a relatively large uncertainty. Moreover, electronic cross-talk affects instrument calibration and Earth view (EV) radiance retrievals for both MODIS instruments. Starting Collection 6.1 (C6.1), the electronic cross-talk between the Terra MODIS photo-voltaic (PV) long-wave infrared (LWIR) TEBs is corrected using coefficients derived from monthly lunar observations [*Xiong et al., 2020; Wilson et al., 2017*]. Earth scene observations have provided useful information for calibration assessments, including inter-sensor comparisons and assessments using ocean, desert, Antarctic Dome Concordia (Dome-C), and deep convective clouds (DCC) measurements [*Xiong et al., 2009; Wenny et al., 2007; Chang et al., 2018; Chang et al., 2019; Chang et al., 2020; Shrestha et al., 2018; Diaz et al., 2019*]. A notable feature of the DCC observations is that the probability density function (PDF) of the 11-μm (MODIS band 31) brightness temperatures (BTs), as well as other TEB BTs, over certain periods of time. Their PDFs are neither Gaussian nor symmetrical and can have effect for the calibration assessment. However, these asymmetrical BT distributions are drastically reduced after normalization, thus improving the statistical analysis' accuracy. This helps the calibration assessments over cold scenes (e.g. Dome-C and DCC) for BT stability and mirror side bias. The calibration assessment over low BT scene can lead to corrections of the offset calibration term. Both the Terra MODIS safe mode (February 2016) and Aqua MODIS formatter reset (January 2018) events had impacts on the instruments' responses and the mirror side difference. Selected Earth scenes have been used for the impact assessments.

This study focuses on the MODIS TEBs calibration assessment using certain Earth scenes or sites. Stability and consistency are evaluated over the entire MODIS instruments' missions. Common artifacts when using Earth scene measurements are seasonal variations and scene-associated non-uniformity. Previous studies have shown that normalizing the data to reference measurements can partially remove these variations [*Xiong et al., 2009; Wenny et al., 2007; Shrestha et al., 2018; Diaz et al., 2019*]. This work expands the use of reference measurements to further enhance the calibration assessment's accuracy over various scene types. The technique used in this work combines the empirical modeling of the relationship between a band and reference temperature measurements to normalize the data. Moreover, a scene's BT dependency can be used to estimate the calibration coefficients correction based on analytical modeling. In this paper, a normalization method is applied to ocean, desert, Dome-C, and DCC measurements prior to the MODIS TEBs calibration assessment. Reference measurements come from band 31 and ground measurements for some sites. Section 2 presents the TEBs calibration assessment modeling background and Earth scene measurements used. Section 3 describes the normalization and BT dependency technique methodology. Section 4 presents the stability and consistency assessments for both MODIS instruments and all TEBs using Dome-C, ocean, and desert measurements. Additionally, the MODIS TEBs calibration assessment results using DCC from our previous work are included for comparisons.

2 Background

2.1 MODIS TEB calibration

The MODIS TEBs include mid-wave infrared (MWIR) bands 20-25 and LWIR bands 27-36. Bands 20-30 consist of ten PV detectors per band, while bands 31-36 consist of ten photo-conductive (PC) detectors per band. All TEB detectors are located on two cold focal plane assemblies (CFPAs): a short-wave and mid-wave infrared (SMWIR) FPA and a LWIR FPA, which are nominally controlled on-orbit at 83 K. The on-board BB serves as the primary calibration source, while the space view (SV) provides a reference for the instrument

background. The MODIS TEBs calibration uses a quadratic algorithm on a scan-by-scan basis for each TEB detector and each side of the scan mirror. The BB WUCD, with a variant temperature ranging from instrument ambient temperature (about 270 K) to 315 K, is used to characterize the instrument nonlinear response coefficients on-orbit. During a nominal operation, the BB temperature is set to 290 K (285 K since late April 2020) for Terra MODIS and 285 K for Aqua, and the response function's linear coefficient is calibrated scan-by-scan, whereas the nonlinear coefficient and offset are obtained from a LUT [*Xiong et al., 2009; Xiong et al., 2015*].

The TEBs calibration quadratic algorithm converts the digital response of the sensor to calibration radiance (L_{CAL}). The calibration radiance from the BB is adjusted for instrument self-emission due to response versus scan angle (RVS) effects,

$$L_{CAL} = RVS_{BB}\varepsilon_{BB}L_{BB} + (RVS_{SV} - RVS_{BB})L_{SM} + RVS_{BB}(1-\varepsilon_{BB})\varepsilon_{cav}L_{cav} \ , \quad (1)$$

where ε is the emissivity of BB and cavity. The radiance from BB, scan mirror, and cavity are denoted as L_{BB}, L_{SM}, and L_{cav}, respectively. A quadratic function, $L_{CAL} = a_0 + b_1 dn_{BB} + a_2 dn_{BB}^2$, is used for the calibration of the instrument response with the offset term a_0, the quadratic term a_2, and the digital response of the BB given in digital counts (dn_{BB}). The linear coefficient for Earth radiance retrievals can be expressed as:

$$b_1 = [RVS_{BB}\varepsilon_{BB}L_{BB} + (RVS_{SV} - RVS_{BB})L_{SM} + RVS_{BB}(1-\varepsilon_{BB})\varepsilon_{cav}L_{CAV} - a_0 - a_2 dn_{BB}^2]/dn_{BB} \quad (2)$$

From this equation, the calibration uncertainty impact on the Level 1B (L1B) product can be modeled. The major calibration errors include: uncertainties in the nonlinear coefficient $\Delta a_2$and offset Δa_0terms, BB emissivity uncertainty $\Delta\varepsilon_{BB}$, and BB temperature measurement biases ΔT_{BB}. Random noise effects, such as noise in the digital output, are not included. These uncertainties propagate to the linear coefficient b_1 and, with the first order effect, its uncertainty can be derived as [*Chang et al., 2019*] :

$$\frac{\Delta b_1}{b_1} = \Delta\varepsilon_{BB}^{eff} - \frac{\Delta a_0}{L_{BB}} - \frac{L_{BB}}{b_1^2}\Delta a_2 \ , \quad (3)$$

where $\Delta\varepsilon_{BB}^{eff} = \Delta\varepsilon_{BB} + \left[\frac{dL(T)}{dT}\right]_{T=T_{BB}}$ for simplification. The EV radiance retrieval uses:

$$L_{EV} = \frac{1}{RVS_{EV}}[a_0 + b_1 dn_{EV} + a_2 dn_{EV}^2 - (RVS_{SV} - RVS_{EV})L_{SM}]. \quad (4)$$

Hence, the impact on the EV retrieval equation with the first order error propagation becomes:

$$\frac{\Delta L_{EV}}{L_{EV}} = \Delta\varepsilon_{BB}^{eff} + (L_{BB} - L_{EV})\left(\frac{\Delta a_0}{L_{EV}L_{BB}} - \frac{\Delta a_2}{b_1^2}\right). \quad (5)$$

Because the BB temperature is fixed during nominal operation, the calibration uncertainty impact is dependent upon the EV BTs. The first term is due to the pre-launch BB emissivity characterization and on-orbit temperature measurement bias; thus its impact on the relative EV radiance bias is constant. The nonlinear response uncertainty impacts, the second and

third terms on Eq. 5, have different EV radiance dependencies. These provide practicability to identify the cause of the bias and support calibration improvements.

2.2 Assessment using Earth measurements

Typical scenes used for the TEBs calibration assessment include Dome-C, the ocean, the desert, and DCC [*Xiong et al., 2009; Wenny et al., 2007; Chang et al., 2019; Chang et al., 2020; Shrestha et al., 2018; Diaz et al., 2019*]. The previously mentioned normalization method is demonstrated using these four EV scene types. Figure 1 shows the geographical locations for each scene type chosen in this work. The MODIS C6.1 L1B data over the entire mission are used for the analyses. Dome-C (75.12 S, 123.395 E) is one of the most homogeneous EV targets, and is commonly used to track the on-orbit calibration of thermal remote sensing satellite instruments [*Xiong et al., 2009; Wenny et al., 2007; Cao et al. 2010; Blonski et al., (2012); Potts et al., 2013*]. The site is a high polar plateau region with a mean elevation of 3200 meters near the Italian-French base of Concordia. Its relative uniformity, long-term stability, dry atmosphere, low aerosol loading and wind speed, low cloud cover, and frequent satellite overpasses make it a useful site to track the calibration stability and consistency of satellite sensors. Due to its location near the Earth's South Pole, both MODIS sensors have multiple overpasses per day. For each selected granule in the study, the radiances of a 20 km x 20 km region-of-interest are retrieved and converted to BT.

The ocean site, located in the North Atlantic Ocean (23.70 N, 41.57 W), and the Libya-4 desert (28.55º N, 23.39 º E) are shown in the top left and right charts in Figure 1, respectively. Both selected regions are 20 km x 20 km in size. Quasi-DCC measurements, developed for the assessment of the TEBs in our previous work, are also used to demonstrate the normalization technique [*Chang et al., 2020*]. Only nighttime measurements are analyzed to avoid the solar reflectance impact on MWIR bands. The DCC pixels are identified as those located over the tropical domain - between latitudes 30° N and 30° S - with BTs lower than 205 K at 11 μm (MODIS TEB 31). Spatial homogeneity thresholds are used to characterize the DCC core. The IR temperature and visible reflectance (0.65-μm; MODIS band 1) standard deviations were computed over all 3 km x 3 km blocks surrounding each potential DCC pixel. Afterwards, if the IR temperature standard deviation (STD) was higher than a-1 K threshold, or the reflectance STD larger than 3 %, the potential DCC pixel was discarded [*Doelling et al., 2004; Doelling et al., 2010; Doelling et al., 2013*]. However, as presented in our previous work, using daytime DCC has constraints over the calibration assessment of the MWIR bands; thus the nighttime quasi-DCC technique is used [*Chang et al., 2019; Chang et al., 2020*]. The visible reflectance homogeneity is ignored due to a lack of nighttime measurements.

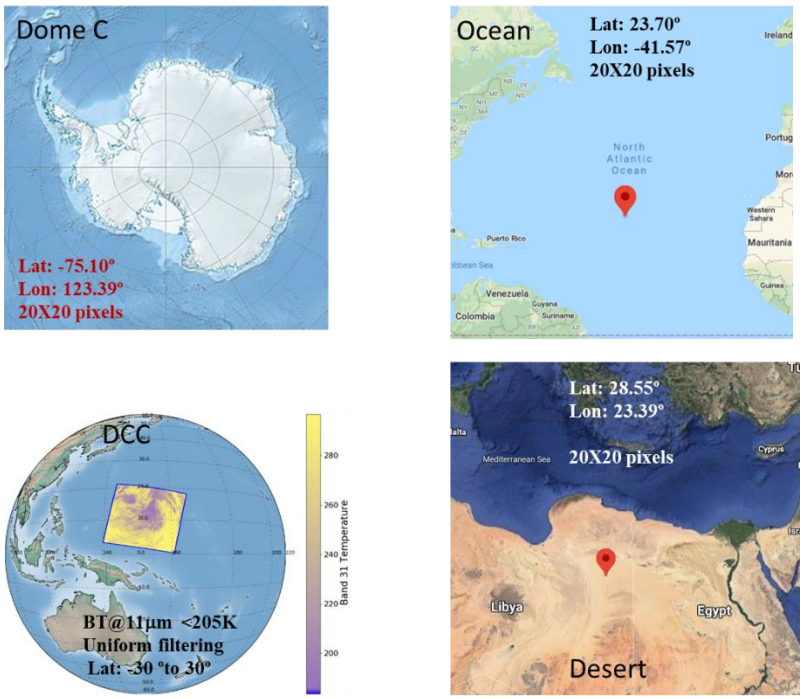

Figure 1. The Earth scenes/sites used for the MODIS TEBs calibration assessment performed in this work. (Dome-C, Ocean, and desert images are from Google Maps)

3 Methodology

3.1 Normalization using empirical modeling

In this work, a normalization method is presented for the TEBs calibration assessment using Earth scenes. Sensor measurements are referenced to those from ground instruments, or from a well-calibrated band. To further enhance the accuracy and derive the BT-dependent correlation, the measurements are normalized to the temperatures of reference measurements. The normalized temperature can be selected as the average of the reference measurements or a key temperature good for the calibration assessment. Generally, the measurements from any given band over an Earth scene have correlation with reference measurements. This relation can be derived using a physical or empirical model. An empirical model is used to describe the correlation between band and reference measurements. The correlation and normalization can be combined into one empirical model as follows:

$$BT_{model}(b) = f\left(BT_{ref} - BT_{ref_{nor}}\right). \quad (6)$$

The dependency function should be determined from various tests over an Earth scene. In this case, a quadratic function is used as the empirical model,

$$BT_{model}(b) = c_0 + c_1\left(BT_{ref} - BT_{ref_{nor}}\right) + c_2\left(BT_{ref} - BT_{ref_{nor}}\right)^2, \quad (7)$$

where $c_{0,1,2}$ are fitting coefficients, BT_{ref} is the reference measurement, and $BT_{ref_{nor}}$ is the normalization temperature of the reference measurements. The fitting coefficients are determined from the model regression dependency. The c_0 fitting coefficient is the band's

normalized Earth scene measurement at the reference BT from the model. Afterwards, the band measurements can be normalized using:

$$BT_{nor}(b) = BT(b) - c_1\left(BT_{ref} - BT_{ref_{nor}}\right) - c_2\left(BT_{ref} - BT_{ref_{nor}}\right)^2 \quad . \tag{8}$$

For equations (7) and (8), it is mathematically equivalent for with reference temperature and without reference temperature. With the temperature in the equations, the first term is the band BT corresponding to the reference temperature of the reference band. As described earlier, this method relies on establishing a relationship between band and reference measurements over a selected scene. The assessment's accuracy depends on the correlation between these measurements. This method may not work for a band with low correlation with its reference over a certain scene. The goal of the normalization is to improve the assessment's accuracy, and to provide calibration assessments at desired signal levels, which is useful as inputs for the calibration assessment's modeling.

This normalization method is different from a simple trending technique that uses the difference between a band and reference band. The method presented in this work normalizes the band's measurement to a reference BT of the reference band with an empirical model. Normally, in order to do this, the band's BT (e.g. typical temperature over the scene) is selected, and its corresponding band 31 BT is calculated from the empirical model. Afterwards, the band 31 BT is used as the reference BT. The technique provides the advantage of trending the band's measurements normalized to approximately the same BT over the whole instrument's mission.

3.2 Cloud filtering and temperature range consideration

Cloud conditions affect scene characterization (e.g. BT range and the correlation between band and reference measurements). The MODIS cloud mask (CM) product (MOD35 for Terra and MYD35 for Aqua) is used to identify and screen the cloudy pixels. The CM product provides both a cloud mask determination flag and cloud mask value for each 1-km pixel. The CM value can range from 0 (cloudy) to 3 (confident clear). The normalization method benefits from a large number of measurement samples and high correlation between band and reference measurements over a broad BT range. However, scene type variations and broader BT ranges may affect these correlations. After numerous cloud screening tests, Figure 2 shows the measurements used in this work. The CM filtering does not apply to the qDCC measurements.

The measurement samples with clear sky show high correlation between each band and band 31 for the ocean, desert, and Dome-C scenes. Moreover, measurement sample number and BT coverage should also be considered in the CM filtering threshold selection. Figure 2 shows the TEB 31 BT histograms for the cloud screened samples with different CM filtering options. Clear sky measurements dominate the Dome-C and desert sites, while cloudy retrievals are predominant over the ocean site. As expected, the clear sky samples predominate Dome-C, and selecting the samples with a CM equal to 3 filters out all measurements with cloudy effects without significantly reducing the BT range and sample number. On the other hand, clear sky measurements are limited for the ocean scene. Hence, selecting measurements with a CM as low as 1 over the ocean scene removes measurements outside the 200 K to 280 K BT range without significantly impacting the sample number. Lastly, a CM threshold of 2 or higher over the desert site removes a small amount of samples within the broad 190 K to 240 K BT range. During the CM threshold selection process, the normalization method application is also taken into consideration. Section 3.3 presents a

detailed discussion on this subject. Lastly, the qDCC are clouds themselves, and thus no CM filtering is needed over qDCC.

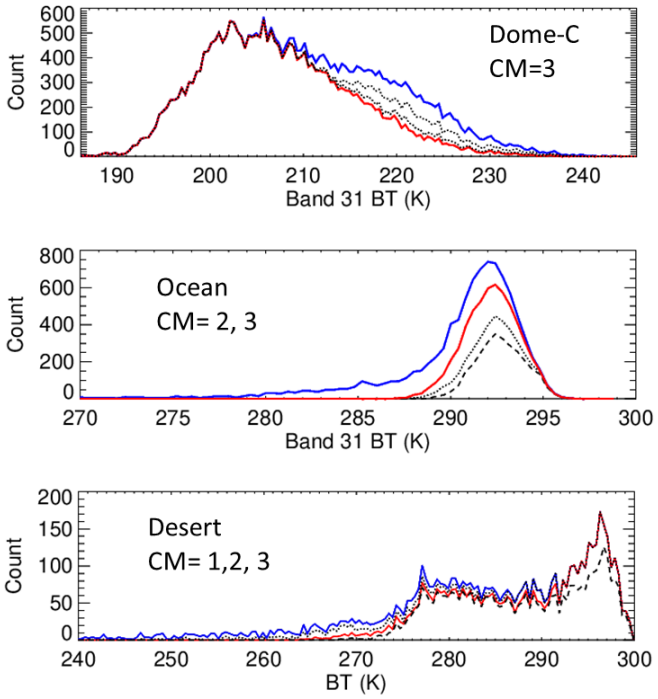

Figure 2. Terra TEB 31 BT measurements distribution over Dome-C, the ocean, and the desert under different CM thresholds. The blue curves represent all the nighttime measurements, and the other three curves are CM ranges from 3 to 1, 3 to 2, and 3 only. The red curves denote the CM-filtered measurements used in this work.

3.3 Considerations when using normalization references

There are significant differences between ground measurements and satellite instrument (e.g. MODIS) retrievals. Firstly, the top-of-atmosphere measurements from satellite instruments are affected by both the atmosphere and cloud conditions - even for those bands designed for Earth surface BT retrievals. Secondly, satellite instruments measure spectral radiance, and then convert to brightness temperature for the corresponding band spectrum. Hence, the scene emissivity is spectrally-dependent and makes the ground temperature measurements and satellite instrument BTs different. Lastly, scene uniformity, seasonal variation, and time difference between measurements have effects on the satellite instrument retrievals. On the other hand, ground measurements have advantages, such as accurate ground instrument calibration and SI traceability.

Measurements from other spectral bands from the same instrument can be used as reference as well. The advantages of using another band as reference include same pixel measurements over near identical geolocations, simultaneous measurements, similar calibration algorithm, and sufficient data. The band specifications of an instrument vary with the design and application accordingly. For example, the MODIS TEB 31 (centered around 11 μm and used primarily for surface and cloud temperature measurements) specification has the stringiest requirement of all MODIS TEBs (NEdT requirement of 0.05 K at typical BT) [*Xiong et al., 2015*]. On-orbit performance shows that the calibration uncertainty for this band is well within the specification. Many MODIS TEBs performance assessments use this band as a

reference. Additionally, for the TEBs performance assessments using DCC, the pixel identification requires the use of TEB 31 BTs [*Doelling et al., 2004; Doelling et al., 2010; Doelling et al., 2013*; *Chang et al., 2019; Chang et al., 2020*]. This band provides assessment advantages when using DCC as a reference – as previously proven when applied to the Aqua MODIS TEBs.

The fitting uncertainty (and correlation with band 31) is band dependent. Thus, the correlation and accuracy of the normalization model can be evaluated using the fitting residual and R^2 of the fit [*Press et. al, 1992*].The top chart of Figure 3 shows the STD of the absolute fitting residuals for the normalization model for the desert measurements and each band. In order to show the spectral features, the STD is shown as a function of each band's center wavelength. Small STD values indicate a good fit, while large STD values denote scattering in the measurements around the model. The bottom chart shows the fit's R^2 values for the desert scene. Table 1 lists the fit's R^2 values for the desert, ocean, and Dome-C scenes for all the Terra and Aqua MODIS TEBs. An R^2 value close to 1 means unity, while naught defines no correlation between the band's measurements and the reference data. Terra and Aqua MODIS show consistent results. For the desert site, bands 27 and 28 show poor correlation with band 31, while the other bands show better correlation. Bands 20-23, 29, 32, and 33 show high correlation with band 31. Similar assessments were made to evaluate the correlation between each band's measurements with the reference band for the other scenes. The goodness of fit is both scene- and band-dependent. Overall, the desert scene shows the best correlations between all bands and reference band 31. The ocean scene shows a low degree of correlation for most bands. However, bands 25, 29, 32, and 33 show relatively large correlations. Any improvement by using the normalization technique will be limited for the bands with low R^2 values over any scene. Nonetheless, this is just one metric that can be used to evaluate the improvements produced by the normalization method.

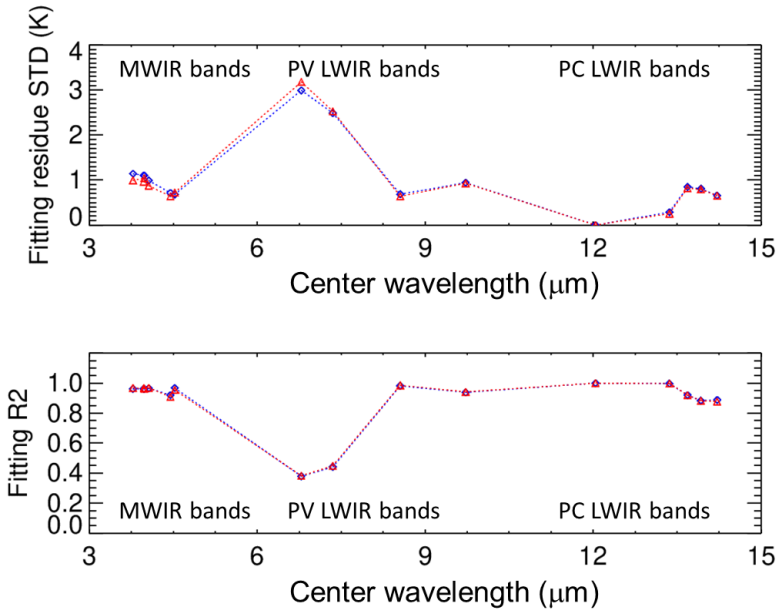

Figure 3. (Top) Standard deviation of the absolute fitting residuals for the normalization model for the desert measurements and each band. In order to show the spectral features, the STD is shown as a function of each band's center wavelength. (Bottom) Fitting model's R^2 over desert measurements for each band with respect to band 31. Samples from the entire

satellite missions are used. Band 31 is not shown in either chart, since it is the reference. Blue and red define Terra and Aqua, respectively.

Table 1. The fitting model's R^2 for each band's measurements with respect to band 31 over the desert, the ocean, and Dome-C for all the Terra and Aqua MODIS TEBs.

Band	Terra R2			Aqua R2		
	Desert	Ocean	Dome-C	Desert	Ocean	Dome-C
20	0.962	0.593	0.950	0.970	0.613	0.936
21	0.962	0.477	0.392	0.962	0.460	0.239
22	0.961	0.470	0.981	0.967	0.472	0.978
23	0.966	0.486	0.974	0.969	0.487	0.967
24	0.920	0.358	0.350	0.909	0.326	0.271
25	0.968	0.569	0.746	0.954	0.509	0.645
27	0.379	0.064	0.602	0.382	0.060	0.624
28	0.441	0.148	0.886	0.448	0.146	0.888
29	0.982	0.938	0.994	0.985	0.945	0.994
30	0.938	0.318	0.503	0.941	0.338	0.486
32	0.997	0.966	0.999	0.997	0.963	0.999
33	0.920	0.705	0.911	0.920	0.713	0.909
34	0.883	0.521	0.669	0.883	0.521	0.676
35	0.888	0.459	0.469	0.877	0.407	0.464
36	0.813	0.239	0.187	0.806	0.192	0.194

4 Application to the MODIS TEBs

4.1 Applications

The normalization technique is applied to assess the TEBs using Earth measurements over Dome-C, the ocean, the desert, and DCC. Among these Earth scenes, DCC are treated and processed differently, while the technique's application to the other scene types is similar after the CM threshold selection. The left panels in Figure 4 show the BTs as a function of the band 31 BTs, and the empirical model applied to Terra TEBs 22, 29, and 35. The empirical model presented in Eq. (7) is used to determine the dependency between the MODIS band BTs using the TEB 31 BTs as reference. The normalization BT is set to the average of the TEB 31 BTs over the entire Terra mission. The right panel charts show the PDF of these bands' BTs, and their PDF after normalization. Band 29 exhibits strong correlation with band 31, and its PDF after normalization has a narrow Gaussian-shaped distribution. Band 22 also shows good correlation with band 31, and exhibits significant distribution improvement; near-Gaussian in shape. On the other hand, band 35 did not show much improvement.

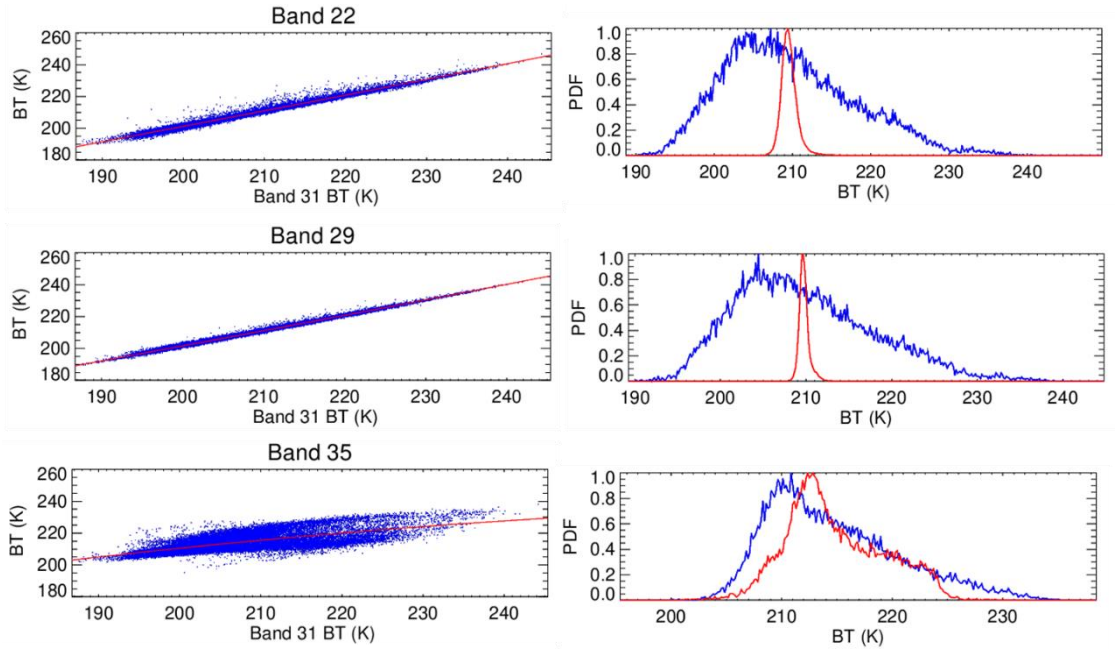

Figure 4. (Left) Terra MODIS mission-long BTs as a function of the MODIS band 31 BTs (blue) and its empirical model (red) for bands 22, 29, and 35 over Dome-C during nighttime. (Right) PDF for MODIS BTs (blue) and its PDF after normalization (red) for the selected bands.

The motivation for developing the normalization technique is to support the TEBs calibration assessments. One major advantage is using a fixed BT or narrow BT range to make the calibration modeling feasible (as presented in Sec. 2.1). Another advantage is to improve the stability assessments' accuracy. In this paper, the improvement when using the normalization is demonstrated using the long-term trending (Sec. 4.2).

Similar analyses were performed over the ocean site for the entire Terra and Aqua MODIS missions. The band 31 BTs are used as reference. The left panels in Figure 5 show the dependency between the band and reference measurements for TEBs 22, 29, and 35. The red lines represent the application of the empirical model (Eq. (7)) using the average band 31 BT as the normalization BT. As stated in section 3.1, it is mathematically equivalent for the regression with a reference temperature and without a reference temperature. By using a reference temperature, the band BT corresponding to the reference temperature of the reference band is the offset term in the regression. It is also helpful to understand the normalization method. The right panels show the BT histograms before and after normalization. Band 29 shows significant improvement after the normalization, while the improvement for band 22 is limited. Due to a lack of correlation with the reference band, band 35 shows unnoticeable improvement.

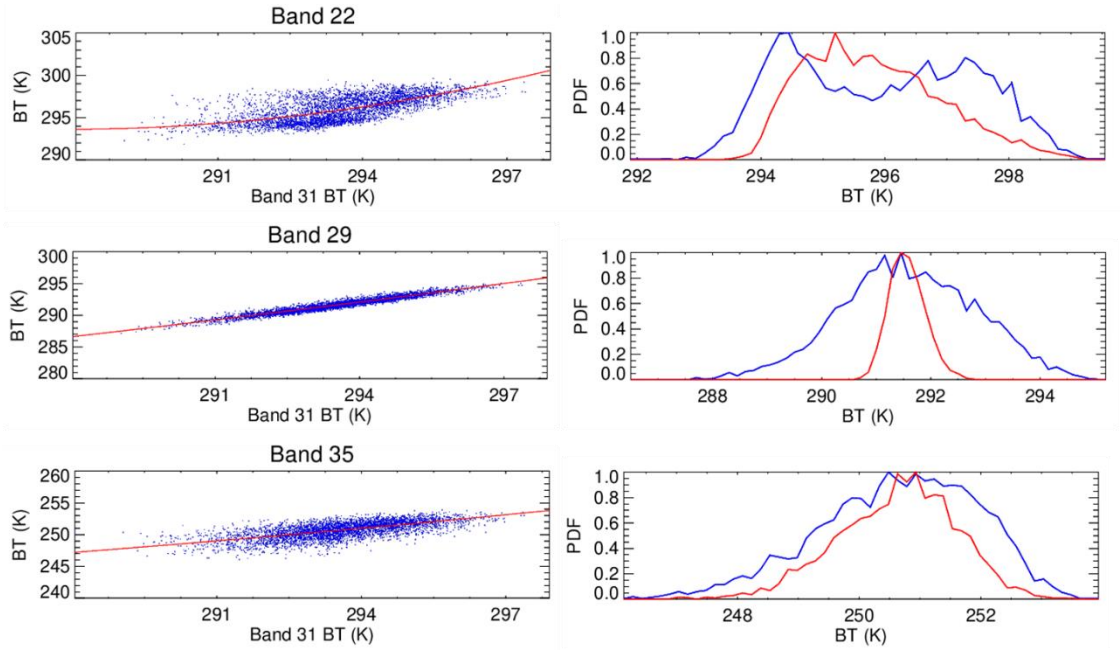

Figure 5. (Left) Terra MODIS mission-long BTs as a function of the MODIS band 31 BTs (blue) and its empirical model (red) for bands 22, 29, and 35 over the ocean site during nighttime. (Right) PDF for MODIS BTs (blue) and its PDF after normalization (red) for the selected bands.

As shown in Sec. 3.3, the majority of the measurements over desert are clear sky, and thus these scenes are frequently used for sensor calibration assessments. The left panels in Figure 6 show the dependency between band and reference measurements for TEBs 22, 29, and 35. The red lines are the application of the empirical model presented in Eq. (7). All three bands have strong correlation with the TEB 31 reference. The right panels show the BT histograms before and after normalization. Band 22 shows significant improvement after the normalization, and its distribution is narrow and Gaussian in shape. The improvement for TEB 29 is also significant, while TEB 35 shows smaller improvement when compared to TEBs 22 and 29.

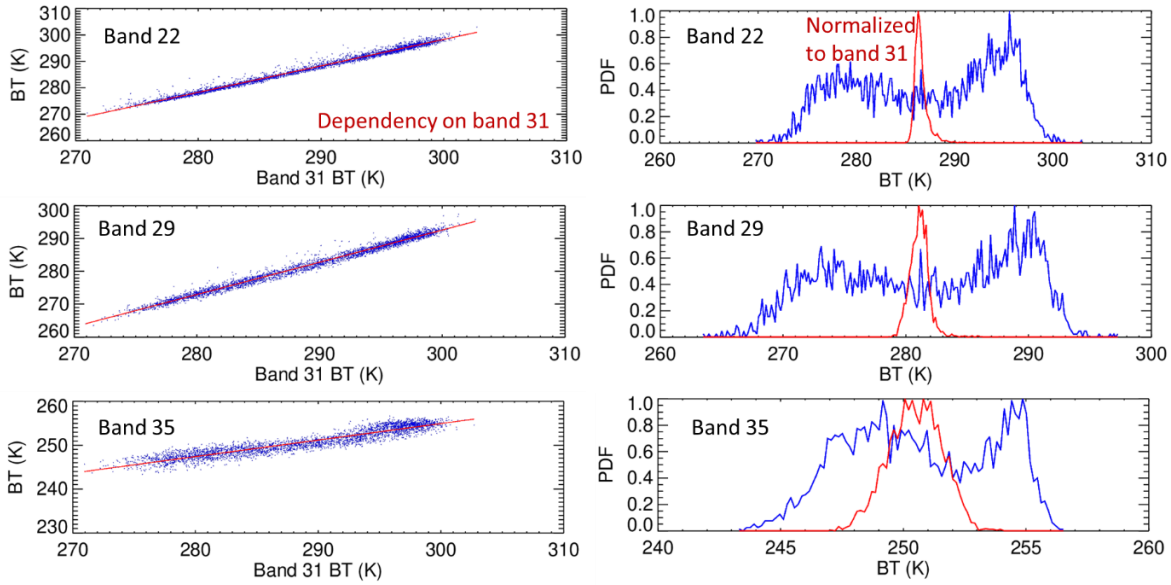

Figure 6. (Left) Terra MODIS mission-long BTs as a function of the MODIS TEB 31 BTs (blue) and its empirical model (red) for bands 22, 29, and 35 over the desert site during nighttime. (Right) PDF for MODIS BTs (blue) and its PDF after normalization (red) for the selected bands.

Due to an enormous number of DCC samples, the normalization process is month-dependent and the average monthly results are used for the calibration assessments. This is not common practice for the other Earth scenes (i.e. Dome-C, ocean, and desert). Figure 7 displays the Aqua MODIS band 31 qDCC BT distribution for January 2019. Band 31 BTs range from 180 K to 205 K, and their distribution reaches its peak around the maximum BT. A broad, cutoff, and non-centered distribution can cause problems for calibration assessments, especially for the low DCC BTs. Moreover, the band 31 BT distribution and DCC sample number varies monthly; causing additional uncertainty to the calibration assessment.

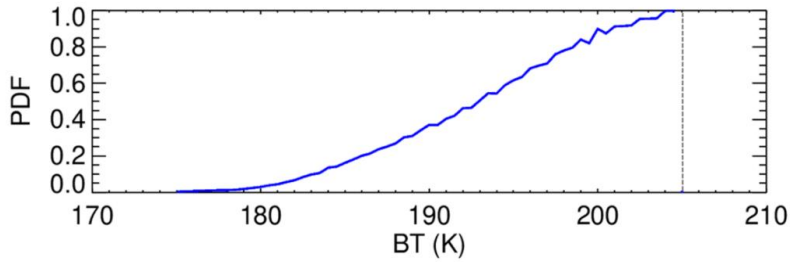

Figure 7. Aqua TEB 31 BTs PDF over nighttime qDCC for January 2019. The dashed line indicates the 205 K BT used for DCC pixel identification.

The left panels in Figure 8 show the BTs as a function of the band 31 BTs over nighttime qDCC for January 2019, and the empirical model for the reference dependency for Aqua MODIS TEBs 22, 29, and 35. Due to the large number of DCC samples, the BTs are binned every temperature degree. The average binned BT and its standard deviation are plotted. The red lines define the empirical model application. The normalization BT is set to a constant

200 K for every month. Bands 29 and 35 show strong correlation with the band 31 measurements. The right panels in the Figure 8 illustrate the bands BTs' PDF before and after normalization for January 2019. Band 22 shows significant improvement in its distribution's shape after the normalization; near-Gaussian. Due to the strong correlation with band 31, the PDFs of bands 29 and 35 are asymmetrical in shape. The normalization makes them symmetrical and narrower.

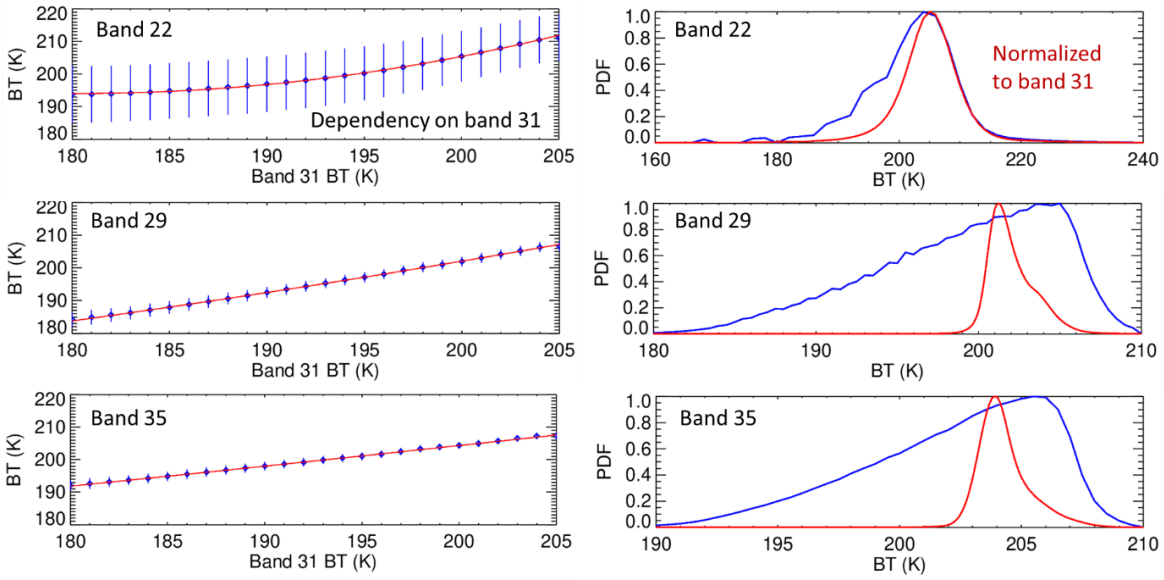

Figure 8. (Left) The BT measurements as a function of the TEB 31 BTs (blue) over nighttime qDCC for January 2019, and the empirical model for the reference dependency (red) for Aqua MODIS TEBs 22, 29, and 35. Due to the large number of DCC samples, the BTs are binned every temperature degree. The average binned BT and its standard deviation are plotted. (Right) PDF of bands BTs before (blue) and after (red) normalization. The normalization BT is set to constant 200 K for the band 31 reference.

4.2 Stability assessments

The normalization method has been applied to perform stability assessments on the Terra and Aqua MODIS TEBs over their entire missions. This paper shows some examples of the analyses and gives a summary table of the stability results. It was found that the stability is BT dependent for some bands. This paper presents some examples of the Aqua TEB assessments using qDCC and Dome-C and Terra TEB assessments using the ocean and desert sites. Bands 22, 29, and 35 are still used to represent all the scenes. The left charts of Figure 9 show the entire mission BT trending for Aqua bands 22, 29, and 35 over the nighttime qDCC. The blue symbols define BTs averaged over each month, while the red symbols represent the bands' BTs after normalization. The normalization band 31 BT is set to 200 K for every month. The monthly average fluctuations are significantly reduced for all bands. Before the normalization, the average band 31 BT varies due to the DCC sample number and monthly distribution variation. This uncertainty propagates to the long-term stability assessment. Moreover, by fixing the normalization reference BT value for band 31, the bands' BTs after normalization can be estimated using the empirical model. Afterwards, these results can be used as input for the calibration assessment model presented in Sec. 2.1. The right charts of Figure 9 show Aqua mission BT trends for bands 22, 29, and 35 over Dome-C during nighttime. Due to the high latitude of Dome-C, there are no night

measurements for some months every year. The blue symbols represent the Dome-C MODIS BTs, while the red symbols define the MODIS BTs after being normalized using the band 31 BTs as reference.

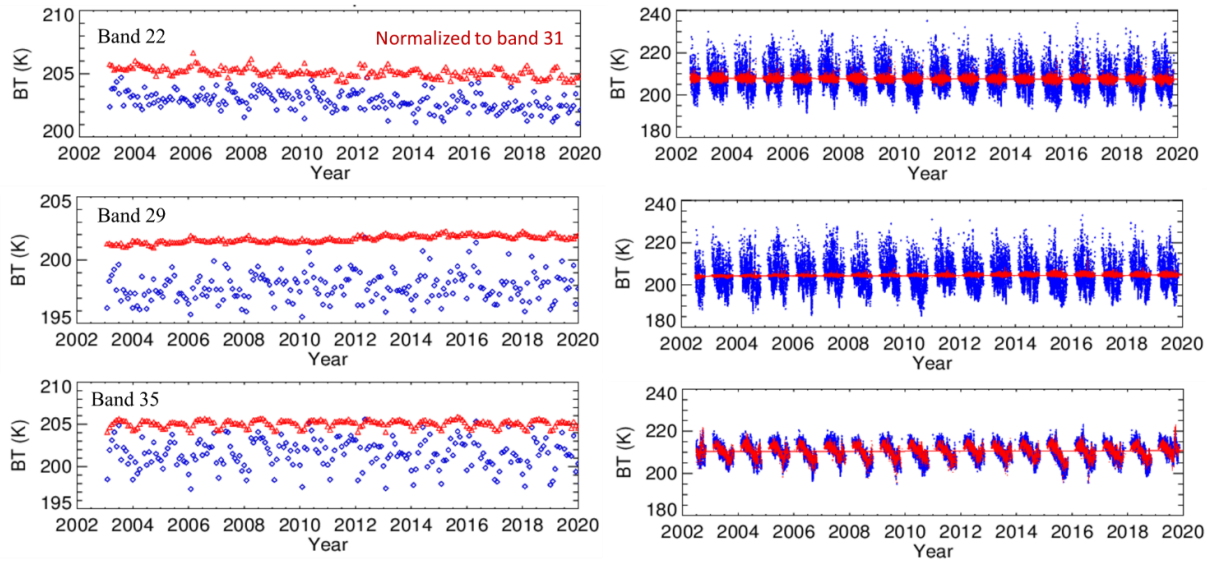

Figure 9. (Left) The entire mission BT trends for Aqua MODIS TEBs 22, 29, and 35 over the nighttime qDCC. The blue symbols define BTs averaged over each month, while the red symbols represent the average BTs after normalization. The normalization band 31 BT is set to 200 K for every month. (Right) Aqua mission BT trends for TEBs 22, 29, and 35 over Dome-C during nighttime. The blue symbols represent Dome-C MODIS BTs, while the red symbols define the MODIS BTs after being normalized using the TEB 31 BTs as reference.

The left charts of Figure 10 show the entire mission BT trends for Terra bands 22, 29, and 35 over the ocean during nighttime, while the right charts show the Terra BT trends for the same bands over the desert site. The blue symbols define BTs averaged over each month, while the red symbols represent the bands' BTs after normalization. The normalization band 31 reference BT is set to its average BT. The monthly average fluctuations are reduced for all bands. However, the improvement is band- and Earth scene-dependent. Both scenes show significant improvements for bands 29, 32, 33. The desert scene shows large improvements for all TEBs - except bands 27 and 28.

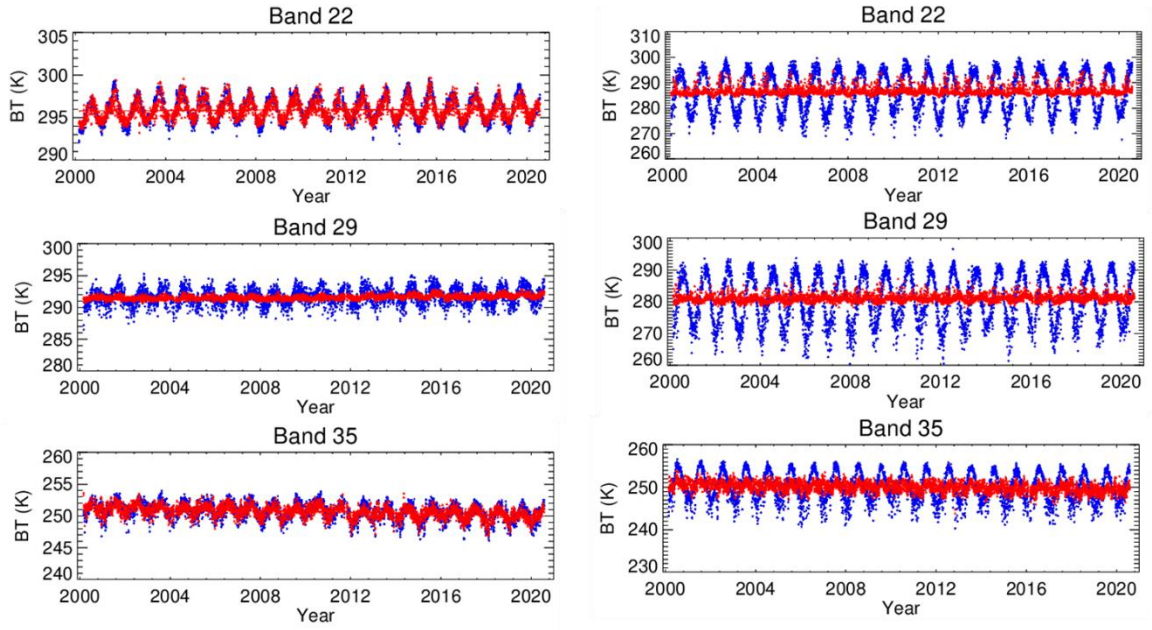

Figure 10. (Left) Terra mission BT trends for TEBs 22, 29, and 35 over the ocean site during nighttime. The blue symbols represent the ocean site MODIS BTs, while the red symbols define the MODIS BTs after being normalized using the TEB 31 BTs as reference. (Right) Terra mission BT trends for TEBs 22, 29, and 35 over the desert site during nighttime. The blue symbols represent the desert site MODIS BTs, while the red symbols define the MODIS BTs after being normalized using the TEB 31 BTs as reference.

As mentioned previously, the advantage of this normalization method is to be able to perform TEB assessments at a fixed band's BT for certain scenes corresponding to band 31's reference BT. For Dome-C, band 31 has been demonstrated to be quite stable and was used as reference for the other bands. This is quite useful when applying an analytical model for calibration corrections. The top chart of Figure 11 displays an example of each band's fixed BT, and this BT's change rate for each instrument's mission at the desert site. The horizontal lines denote the reference BT of band 31 and the markers define the band's corresponding BT. There is a slight difference between the Terra and Aqua MODIS TEB BTs over the desert site. However, the relative difference between each band and band 31 are consistent for both instruments. The bottom chart of Figure 11 shows the mission-long BT change rate for each band. For both Terra and Aqua, bands 20, 22, 23, 32, and 33 have been stable over their missions. Bands 24, 25, 29, and 34-36 all show downward trends, and both the Terra and Aqua MODIS TEBs display consistent change rates. However, for the PV LWIR bands 27, 28, and 30, Terra and Aqua show different trends. Both the Terra and Aqua band 30 results show downward trends. However, the Terra change rate is approximately twice that of Aqua.

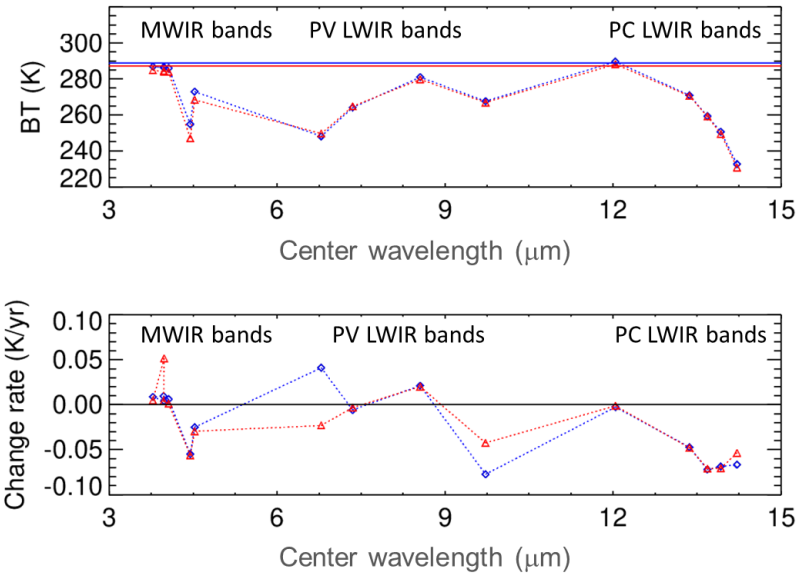

Figure 11. (Top) BT for each band corresponding to the reference BT of band 31 over the desert site. The horizontal lines represent the band 31's BT. (Bottom) The mission-long BT change rate for each band. The BT and BT change rates are plotted at each band's center wavelength. Blue and red define Terra and Aqua MODIS, respectively.

Table 2 summarizes the change rate for all MODIS TEBs and both instruments from the stability assessment over all four scenes during nighttime. Terra MODIS band 30 shows the largest change rate, which is consistent with another study [*Chang et al. 2019*]. The Terra PV LWIR bands are affected by electronic cross-talk, and its effect is characterized and corrected using lunar measurements in C6.1 [*Wilson et al., 2017*]. The downward trend may be partially due to some uncorrected cross-talk residuals during the cross-talk correction. Aqua MODIS band 30 also exhibits a slight, downward trend. The cloud-top property and carbon dioxide bands 34 to 36 exhibit approximately the same downward change rate for both the ocean and desert scenes and both instruments [*Baum et al., 2012; Liu et al., 2020*]. On the other hand, the Dome-C and qDCC scenes show different performances. Dome-C displays a slight, upward trend, while qDCC indicates a stable trend. The atmospheric temperature bands 24 and 25, and cloud top altitude band 33, exhibit similar performance for both instruments. As shown in Figure 11, these bands' BT measurements are all relatively low. All other TEBs display stable trends (with change rates smaller than 0.040 K/yr; which amounts to roughly 0.8 K) over the instruments' entire missions. The stability can be scene- and BT-dependent. Dome-C and qDCC are cold scenes with negligible atmospheric effects, which is why measurements over these scenes are generally used to assess the offset term in the calibration equation.

As discussed in other literature [*Moeller et al. 2003; Moeller et al. 2014; Liu et al., 2020*], some bands are affected by carbon dioxide (CO_2) absorption as the thermal radiation is transmitted through the atmosphere. The bands with the most CO_2 absorption effects are MODIS LWIR bands 33-36. As the CO_2 level increases, its absorption can cause the measurements from these bands to trend downward. For comparison, the measurements over DCC have insignificant atmospheric and CO_2 absorption effects. Thus, these bands' measurements over DCC show quite stable trends over both instruments' missions. The

nighttime, clear sky Dome-C measurements also have minor atmospheric effects. Hence, the change rates over Dome-C are close to those from the DCC for these bands. Moreover, both Terra and Aqua MODIS show consistent change rates for these bands. Therefore, when using Earth measurements for calibration assessments, climate condition changes, such as CO_2 absorption changes, should be considered.

Band 30 shows a downward trend for both Terra and Aqua MODIS over all scene types. It is also observed that the rate of change in Aqua MODIS band 30 is approximately half of that of Terra MODIS for the ocean, the desert, and Dome-C. The rate of change from DCC for Terra MODIS is much larger when compared to the other scene types (3.5 K lower from mission beginning, whereas 1.2 K and 1.8 K downward drifts are observed for the desert and ocean scenes). Terra MODIS band 30 undergoes larger electronic cross-talk effects when compared to the other PV LWIR bands. Cross-talk correction coefficients are derived from lunar observations, and the correction is applied to the BB calibration and Earth radiance retrievals. Sending signals come from bands 27, 28, and 29, and cross-talk effects are scene- and BT-dependent. Thus, the correction may contain residues for various scenes and BT measurements. A similar Terra band 30 downward trend has been observed from inter-comparisons and the cause of the trend is under investigation.

Table 2. Mission-long BT change rates for all Terra and Aqua MODIS TEBs over the desert, the ocean, Dome-C, and qDCC.

Band	Terra change rate (K/yr)				Aqua change rate (K/yr)			
	Desert	Ocean	Dome-C	qDCC	Desert	Ocean	Dome-C	qDCC
20	0.009	0.002	0.003	-0.014	0.005	-0.008	-0.017	-0.028
21	0.004	-0.004	0.006	0.005	0.051	0.014	0.047	0.020
22	0.009	0.004	0.007	-0.027	0.004	-0.010	-0.030	-0.039
23	0.006	0.001	-0.003	-0.026	0.001	0.010	-0.0289	-0.042
24	-0.055	-0.065	-0.010	-0.014	-0.056	-0.063	-0.014	-0.004
25	-0.025	-0.032	0.001	-0.008	-0.030	-0.037	0.002	0.004
27	0.041	0.022	-0.004	0.042	-0.023	-0.016	-0.008	-0.017
28	-0.006	-0.031	-0.006	0.011	-0.003	-0.002	-0.010	-0.016
29	0.021	0.030	0.022	0.042	0.020	0.022	0.025	0.043
30	-0.077	-0.083	-0.064	-0.175	-0.042	-0.036	-0.018	-0.045
32	-0.003	-0.001	0.006	0.011	-0.001	0.001	0.004	0.008
33	-0.047	-0.046	0.006	0.002	-0.048	-0.044	0.009	0.004
34	-0.072	-0.075	0.003	-0.002	-0.071	-0.070	0.009	0.003
35	-0.069	-0.071	-0.003	-0.005	-0.071	-0.071	0.001	0.002
36	-0.067	-0.074	-0.024	-0.012	-0.053	-0.056	-0.009	0.004

5 Summary

A normalization method is presented for the assessment of the TEBs using Earth scenes, and the TEB long-term trending results by means of calibration stability assessments are demonstrated. The technique has been tested over Dome-C, the ocean, the desert, and

qDCC for all MODIS TEBs. Band 31 measurements are used as references for all four scenes. Results are correlation- (band *vs.* reference) and scene-dependent. Two main motivations were used for the normalization methodology development: 1) to enhance the calibration assessment accuracy by reducing the fluctuations and seasonal variations in the data and 2) to get the calibration assessments at a desired signal level to be used as inputs for the calibration assessment modeling and correction. This paper focuses on the normalization method's development and application demonstration. The technique will be used in future work to support MODIS TEBs calibration assessments.

Most Terra and Aqua MODIS TEBs show mission-long stable trends. Terra band 30 shows the largest downward trend. This issue is under investigation. Aqua band 30 also shows a downward trend, albeit with a much lower change rate. The bands with the largest CO_2 absorption effects show downward trends over the ocean and desert scenes for both Terra and Aqua MODIS. Furthermore, these CO_2 bands' change rates are consistent for the two instruments. However, qDCC and Dome-C, the scenes subjected to smaller CO_2 absorption effects, show more stable trends for both instruments. The downward trend of the CO_2 bands may be due to increases in CO_2 absorption over the ocean and desert scenes for both instruments. Therefore, different types of scenes and broad BT ranges should be used for calibration assessments in order to identify the effects of climate condition changes (e.g CO_2 absorption changes).

Acknowledgments

The authors would like to thank Aisheng Wu and Amit Angal for the internal reviews of this manuscript. The authors would also like to thank other members of the MODIS Characterization Support Team for their technical assistance and contributions made in support of the MODIS long-term calibration and characterization.

All the data used in this paper are available to the public through the Level-1 and Atmosphere Archive & Distribution System (LAADS) Distributed Active Archive Center (DAAC) in the Goddard Space Flight Center (https://ladsweb.modaps.eosdis.nasa.gov). The MODIS Collection 6.1 L1B (MOD021KM for Terra MODIS and MYD021KM for Aqua MODIS), geo-location (MOD03 for Terra and MYD03 for Aqua), and cloud mask data (MOD35_L2 for Terra and MYD35_L2 for Aqua) are selected.

References

Baum, B. A., W. P. Menzel, R. A. Frey, D. C. Tobin, R. E. Holz, S. A. Ackerman, A. K. Heidinger, P. Yang (2012), "MODIS cloud-top property refinements for Collection 6," J. Appl. Meteorol. Climatol. 51(6), 1145–1163

Blonski, S., C. Cao, S. Uprety and X. Shao, (2012) "Using antarctic Dome C site and simultaneous nadir overpass observations for monitoring radiometric performance of NPP VIIRS instrument," IEEE International Geoscience and Remote Sensing Symposium, Munich, 2012, pp. 1061-1064, doi: 10.1109/IGARSS.2012.6351367.

Cao, C., S. Uprety, X. Xiong, A. Wu, P. Jing, D. Smith, G. Chander, N. Fox, S. Ungar (2010). "Establishing the Antarctic Dome C community reference standard site towards consistent measurements from Earth observation satellites" Canadian Journal of Remote Sensing. 36. 498-513. 10.5589/m10-075.

Chang, T., X. Xiong, and A. Angal (2019), "Terra and Aqua MODIS TEB intercomparison using Himawari-8/AHI as reference", J. of Applied Remote Sensing, 13(1), 017501

607 Chang, T., Xiong, X. and Shrestha, A. (2019), “Assessment of MODIS thermal emissive
608 bands calibration performance using deep convective clouds,” JARS 13(4), 044526

609 Chang, T., X. Xiong, A. Shrestha, and P. C. Diaz (2020), "Methodology development for
610 calibration assessment using quasi-deep convective clouds with application to Aqua
611 MODIS TEB", Earth and Space Science, vol. 7, issue 1, pp. 1-15

612 Diaz, C. P. , X. Xiong, and A. Wu (2019), "MODIS thermal emissive bands calibration
613 stability using in-situ ocean targets and remotely-sensed SST retrievals provided by
614 the group for high resolution sea surface temperature", Proc. SPIE 11014, Ocean
615 Sensing and Monitoring XI, vol. 110140, pp. 110140P.

616 Doelling, D. R., L. Nguyen, P. Minnis (2004), “On the use of deep convective clouds to
617 calibrate AVHRR data”, in Proc. SPIE, Earth Observing Systems IX, pp. 281-299

618 Doelling, D.R., G. Hong, D. Morstad, R. Bhatt, A. Gopalan, and X. Xiong (2010), “The
619 Characterization of Deep Convective Cloud Albedo as a Calibration Target Using
620 MODIS Reflectances”, in Proc. SPIE, Earth Observing Missions and Sensors:
621 Development, Implementation, and Characterization, vol. 7862, 78620I-1 to 78620I-
622 10

623 Doelling, D. R., D. Morstad, B. R. Scarino, R. Bhatt, and A. Gopalan (2013), “The
624 Characterization of Deep Convective Clouds as an Invariant Calibration Target and as
625 a Visible Calibration Technique”, IEEE Transactions on Geoscience and Remote
626 Sensing, vol. 51, issue. 3, pp. 1147-1150

627 Liu, T. C., X. Xiong, X. Shao, Y. Chen, A. Wu, T. Chang, and A. Shrestha (2020), “Long
628 term stability monitoring of Aqua MODIS thermal emissive bands through radiative
629 transfer modeling”, Proceedings Volume 11501, Earth Observing Systems XXV;
630 115011K (2020) https://doi.org/10.1117/12.2568052

631 Moeller, C., H. E. Revercomb, S. A. Ackerman, W. P. Menzel, R. O. Knuteson, (2003)
632 “Evaluation of MODIS thermal IR band L1B radiances during SAFARI 2000”, J.
633 Geophys. Res., 108, 8494, doi:10.1029/2002JD002323.

634 Moeller, C., W. P. Menzel, and G. Quinn, (2014) “Review of Terra MODIS thermal emissive
635 band L1B radiometric performance” Proceedings Volume 9218, Earth Observing
636 Systems XIX; 92180T. https://doi.org/10.1117/12.2062138

637 Potts, R. D., S. Mackin, (2013) “Sensor Intercalibration over Dome C for the ESA
638 GlobAlbedo Project”, IEEE Transactions on Geoscience and Remote Sensing
639 51(3):1139-1146, DOI: 10.1109/TGRS.2012.2217749

640 Press, W. H., B. P. Flannery, S. Teukolsky, and W. T. Vetterling (1992), “Numerical Recipes
641 in C: The Art of Scientific Computing”, Cambridge University Press

642 Shrestha, A., A. Wu, and X. Xiong (2018), “Evaluating calibration consistency of Terra and
643 Aqua MODIS LWIR PV bands using Dome C”, Proc. SPIE”, 10644, 106440N

644 Wenny, B. and X. Xiong (2007), "Monitoring MODIS thermal emissive band stability
645 through brightness temperature trending of a ground target, Earth Observing Systems
646 XII", Proc. SPIE, vol. 6677, no. 66770M

647 Wilson, T., A. Wu, A. Shrestha, X. Geng, Z. Wang, C. Moeller, R. Frey, and X. Xiong
648 (2017), "Development and Implementation of an Electronic Crosstalk Correction for
649 Bands 27–30 in Terra MODIS Collection 6", Remote Sensing, vol. 9(6), issue 569

Xiong, X., B. Wenny, A. Wu, and V. Salomonson (2009), "Aqua MODIS Thermal Emissive Bands On-orbit Calibration, Characterization, and Performance", IEEE Trans. Geosci. Remote Sens., vol. 47, issue 3, pp. 803-814

Xiong, X., A. Wu, and B. Wenny (2009), "Using Dome C for MODIS Calibration Stability and Consistency", J. Appl. Remote Sens., vol. 3, no. 033520, 2009.

Xiong, X., A. Wu, B. N. Wenny, S. Madhavan, Z. Wang, Y. Li, N. Chen, W. Barnes, and V. Salomonson (2015), "Terra and Aqua MODIS Thermal Emissive Bands On-Orbit Calibration and Performance", IEEE Transactions on Geoscience and Remote Sensing, vol. 53, issue 10, pp. 5709 - 5721

Xiong, X., E. Aldoretta, A. Angal, T. Chang, X. Geng, D. Link, V. Salomonson, K. Twedt, and A. Wu (2020), **"**Terra MODIS: 20 years of on-orbit calibration and performance**"**, *Journal of Applied Remote Sensing*, vol. 14(3), pp. 037501